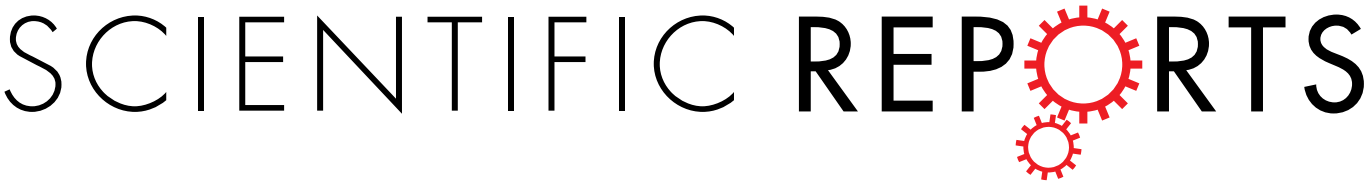

OPEN

Lithium-Decorated Borospherene B_{40}: A Promising Hydrogen Storage Medium

Received: 24 May 2016
Accepted: 26 September 2016
Published: 18 October 2016

Hui Bai[1], Bing Bai[1], Lin Zhang[1], Wei Huang[1], Yue-Wen Mu[2], Hua-Jin Zhai[2,3] & Si-Dian Li[2]

The recent discovery of borospherene B_{40} marks the onset of a new kind of boron-based nanostructures akin to the C_{60} buckyball, offering opportunities to explore materials applications of nanoboron. Here we report on the feasibility of Li-decorated B_{40} for hydrogen storage using the DFT calculations. The B_{40} cluster has an overall shape of cube-like cage with six hexagonal and heptagonal holes and eight close-packing B_6 triangles. Our computational data show that Li_m&B_{40}(1–3) complexes bound up to three H_2 molecules per Li site with an adsorption energy (AE) of 0.11–0.25 eV/H_2, ideal for reversible hydrogen storage and release. The bonding features charge transfer from Li to B_{40}. The first 18 H_2 in Li_6&B_{40}(3) possess an AE of 0.11–0.18 eV, corresponding to a gravimetric density of 7.1 wt%. The eight triangular B_6 corners are shown as well to be good sites for Li-decoration and H_2 adsorption. In a desirable case of Li_{14}&B_{40}-42 H_2(8), a total of 42 H_2 molecules are adsorbed with an AE of 0.32 eV/H_2 for the first 14 H_2 and 0.12 eV/H_2 for the third 14 H_2. A maximum gravimetric density of 13.8 wt% is achieved in 8. The Li-B_{40}-$n$$H_2$ system differs markedly from the previous Li-C_{60}-$n$$H_2$ and Ti-B_{40}-$n$$H_2$ complexes.

Due to its merits of cleanness, renewability, abundance in nature, and high energy density per unit mass, hydrogen has been recognized as an appealing energy carrier for the future world. It has the potential to reduce our dependence on fossil fuels, which are limited in resource and harmful to the environment[1–4]. One bottleneck of using hydrogen for vehicular applications is the lack of safe and efficient hydrogen storage materials[5–7] that store molecular H_2 reversibly with high gravimetric density and fast kinetics for adsorption, as well as desorption, under the conditions of moderate temperature and pressure[8,9]. An ideal H_2 storage system would be one that binds hydrogen in molecular form and with an adsorption energy (AE) in the regime of 0.1–0.5 eV per H_2, that is, intermediate between the physisorbed and chemisorbed states[10,11]. Although advances have been made towards meeting the U.S. DOE's targets for hydrogen storage, an ideal system is yet to be designed and synthesized. Therefore, seeking novel hydrogen storage materials has remained an important issue.

Previous experiments and theoretical calculations have shown that metal-decorated carbon fullerenes and nanotubes[12–19], as well as their boron-, nitrogen- and beryllium-substituted nanostructures[20–22], might be good candidates for the storage of H_2 molecules. For instance, Zhang and co-workers showed that the reversible hydrogen storage of transition-metal-coated C_{60} and $C_{48}B_{12}$ may be as high as 9 wt%[21]. Yildirim *et al.* revealed that Ti-coated single-walled carbon nanotubes can store 8 wt% of H_2[23]. To avoid the clustering problem of transition metal atoms on the surface of carbon nanostructures, Yoon and co-workers[18] found that Ca can achieve homogeneous monolayer coating, which is superior to other metal elements. They concluded that up to 8.4 wt% of hydrogen can be stored in $Ca_{32}C_{60}$ with an AE of 0.2–0.4 eV/H_2. Through first-principles computations, Sun *et al.*[13] predicted that Li-decorated fullerene C_{60} ($Li_{12}C_{60}$) can store up to 9 wt% of H_2, albeit with a rather weak AE of 0.075 eV/H_2. Furthermore, Yoshida *et al.*[17] measured the hydrogen absorption of Li_9C_{60} based on experiments and confirmed that up to ~2.6 wt % H_2 can be stored at 250 °C and 30 bar H_2. For lithium-doped fullerenes (Li_x-C_{60}-H_y) with a Li:C_{60} mole ratio of 6:1, a reversible uptake of 5 wt% H_2 at 350 °C and 105 bar H_2 and desorption onset temperature of ~270 °C was observed[15]. Subsequently, another experimental results[16] showed that up to 9.5 wt % deuterium (D_2) are absorbed in $Li_{12}C_{60}$ under a pressure of 190 bar and a temperature below 100 °C.

[1]Key Laboratory of Coal Science and Technology of Ministry of Education and Shanxi Province, Taiyuan University of Technology, Taiyuan 030024, Shanxi, China. [2]Nanocluster Laboratory, Institute of Molecular Science, Shanxi University, Taiyuan 030006, Shanxi, China. [3]State Key Laboratory of Quantum Optics and Quantum Optics Devices, Shanxi University, Taiyuan 030006, Shanxi, China. Correspondence and requests for materials should be addressed to W.H. (email: huangwei@tyut.edu.cn) or H.-J.Z. (email: hj.zhai@sxu.edu.cn)

Boron is the lighter neighbor of carbon in the periodic table, which possesses the similar merit as carbon in terms of light weight and potential applications for hydrogen storage. For this purpose, its chemical hydrides[24–26] were studied, as were relevant model nanostructures, such as boron monolayer sheets, fullerenes, and nanotubes[27–29]. In particular, following the proposal of the celebrated I_h B_{80} buckyball[30], which is built upon the C_{60} motif by capping all 20 surface hexagons, a number of papers were devoted to hydrogen storage using B_{80} coated with metals (M = Li, Na, K, Be, Mg, Ca, Sc, Ti, and V)[27,31–33]. However, B_{80} was subsequently found to favor core-shell type structures at various theoretical levels[34,35]. It is thus not feasible to pursue any realistic technological applications of B_{80} buckyball as hydrogen storage materials.

Very recently, the first all-boron fullerenes or borospherenes, D_{2d} B_{40} and D_{2d} B_{40}^-, were observed in a combined experimental and theoretical study[36], marking the onset of the borospherene chemistry, whose future development may be envisioned to parallel that of the fullerenes. Endohedral M@B_{40} (M = Ca, Sr) and exohedral M&B_{40} (M = Be, Mg) metalloborospherenes were also predicted, which further support the structural, electronic, and chemical robustness of the B_{40} borospherene[37]. Closely following B_{40}, chiral B_{39}^-, B_{41}^+, and B_{42}^{2+} borospherenes were also studied[38,39], which expand the borospherene family and may eventually lead to new boron-based nanomaterials.

Borospherene B_{40} possesses a cube-like cage structure, whose six hexagonal and heptagonal holes each occupy a face of the cube. It also has eight triangular, close-packing B_6 structural blocks, each on an apex of the cube. All B atoms are on the surface of the cage, which is an ideal, well-defined system for chemistry. B_{40} differs from carbon fullerenes in terms of structure and bonding, and the pursuit of borospherene-based nanomaterials for hydrogen storage is thus intriguing from a fundamental point-of-view. Furthermore, borospherenes are lighter than carbon fullerenes, which make the former systems better candidates to reach a higher gravimetric capacity for hydrogen storage. Relevant to this topic, Dong *et al.*[40] predicted on the basis of density-functional theory (DFT) calculations that Ti-decorated B_{40} fullerene (Ti_6B_{40}) is capable of storing up to 34 H_2 molecules with a maximum gravimetric density of 8.7 wt% and a reversible storage capacity of 6.1 wt%. To our knowledge, the U.S. DOE has set a target of 7.5 wt% for hydrogen storage capacity for the year of 2015[41,42].

In this work, we choose to study lithium-decorated borospherene B_{40} as a potential candidate for hydrogen storage via extensive DFT calculations. Since boron-based nanomaterials are also candidates for lithium storage, the current ternary B-Li-H system is quite unique[28,29,43,44]. Compared to transition metal, Li as the lightest metal definitely will facilitate the improvement of hydrogen storage capacity for the metal-decorated B_{40} system. The Li_m-B_{40}-nH_2 system differs markedly from Li_m-C_{60}-nH_2 or Ti_6-B_{40}-nH_2, which have an AE value that is either rather small (0.075 eV)[13] or too large (up to 0.82 eV)[40]. Even the recently proposed Li_8-B_6-nH_2 system[44] only has an AE of less than 0.1 eV. Our computational data show that Li-decorated B_{40} appears to be a promising medium for hydrogen storage. The Li atoms readily attach to the top of hexagonal and heptagonal holes on B_{40}, forming a series of charge-transfer complexes from C_s Li&B_{40}(**1**), C_{2v} Li&B_{40}(**2**), up to D_{2d} Li_6&B_{40}(**3**). The Li_m&B_{40} complexes can adsorb three H_2 molecules per Li site with a moderate AE of 0.11–0.25 eV/H_2. The Li_6&B_{40}(**3**) complex stores up to 34 H_2 with an average AE of 0.10 eV/H_2. The first 18 H_2 of these possess ideal AEs, which suggest a gravimetric density of 7.1 wt%. Furthermore, the eight close-packing, triangular B_6 corner sites of B_{40} are also suitable for Li-decoration and H_2 adsorption. In a desirable Li_{14}&B_{40}(**7**) complex, up to 42 H_2 molecules can be stored with AEs of 0.12–0.32 eV/H_2, which corresponds to a gravimetric density of 13.8 wt%.

Results and Discussion

Isolated B_{40} Borospherene for H_2 Adsorption. The first all-boron fullerene called as borospherene[36], D_{2d} B_{40} ($^1A_1$), possesses a very large HOMO–LUMO gap of 3.13 eV at the PBE0 level that indicates its overwhelming stability, which is comparable to that of I_h C_{60} (^1A_g) (3.02 eV) calculated at the same level. All the valence electrons in B_{40} are either delocalized σ or π bonds and there is no localized 2c–2e bond, unlike the C_{60} fullerene. In fact, the surface of B_{40} is not perfectly smooth and exhibits unusual heptagonal faces which may play a role that release the surface strains, in contrast to C_{60} fullerene whose surface makes up of pentagons and hexagons and presents the least strain. And the diameter of B_{40} is 6.2 Å, slightly smaller than the value of C_{60} (7.1 Å), which makes B_{40} more comfortable to accommodate a range of small molecules inside the cage.

We initially studied H_2 adsorption on the isolated B_{40} borospherene. The optimized structures of $B_{40}H_2$, H_2@B_{40} and $2H_2$@B_{40} are shown in Fig. 1. In the C_2 $B_{40}H_2$ dihydride, the H_2 molecule tends to form two B–H covalent bonds with the tetracoordinate-B sites, which dissociate H_2. The dissociative AE of a single H_2 is up to 1.30 eV. For H_2 storage inside the cage, only one H_2 molecule can be encapsulated into B_{40}, which is marginally exothermal with an AE of 0.24 eV. Interestingly, once such an encapsulation is completed, the H_2 molecule cannot escape due to substantial energy barriers (>3 eV). The AE of a second H_2 inside the cage is found to be endothermic by 1.32 eV, which is thus not feasible experimentally. In short, the above results show that an isolated B_{40} borospherene is not a good candidate for hydrogen storage directly. The B_{40}-H_2 interactions appear to be different from the case of C_{60}. The latter is known to interact with H_2 via weak van der Waals forces[45]. As a comparison, our calculation results show that the dissociative AE of a single H_2 for $C_{60}H_2$ is only ~0.18 eV at the same level. However, similar to B_{40}, only one hydrogen molecule can reside inside the C_{60} cage with a negative AE value of ~0.22 eV.

Configurations of Li-Decorated B_{40}. As shown in Fig. 2, we start with a single Li atom interacting with B_{40}. Relative stability of Li atom bound on heptagonal and hexagonal holes were considered. The exohedral C_s Li&B_{40}(**1**), in which Li caps a heptagon, turns out to be more stable by 0.20 eV with respect to C_{2v} Li&B_{40}(**2**). In the latter species, Li caps a hexagon. The BE for Li is 3.08 and 2.88 eV in **1** and **2**, respectively. Thus, Li prefers to bind on top of the heptagonal hole of B_{40}. The Li–B distance in **1** is 2.34 Å, compared to 2.33 Å in **2** (Table 1). Clearly, the BE of Li on the center of heptagon or hexagon in B_{40} is substantially higher than those on the pentagon of C_{60} (1.80 eV), in Li_2 dimer (0.95 eV), and in the Li bulk (1.63 eV)[13]. This should help suppress the potency of Li aggregation to form clusters on B_{40} surface, suggesting that Li is a suitable adsorbate to decorate B_{40}. As shown

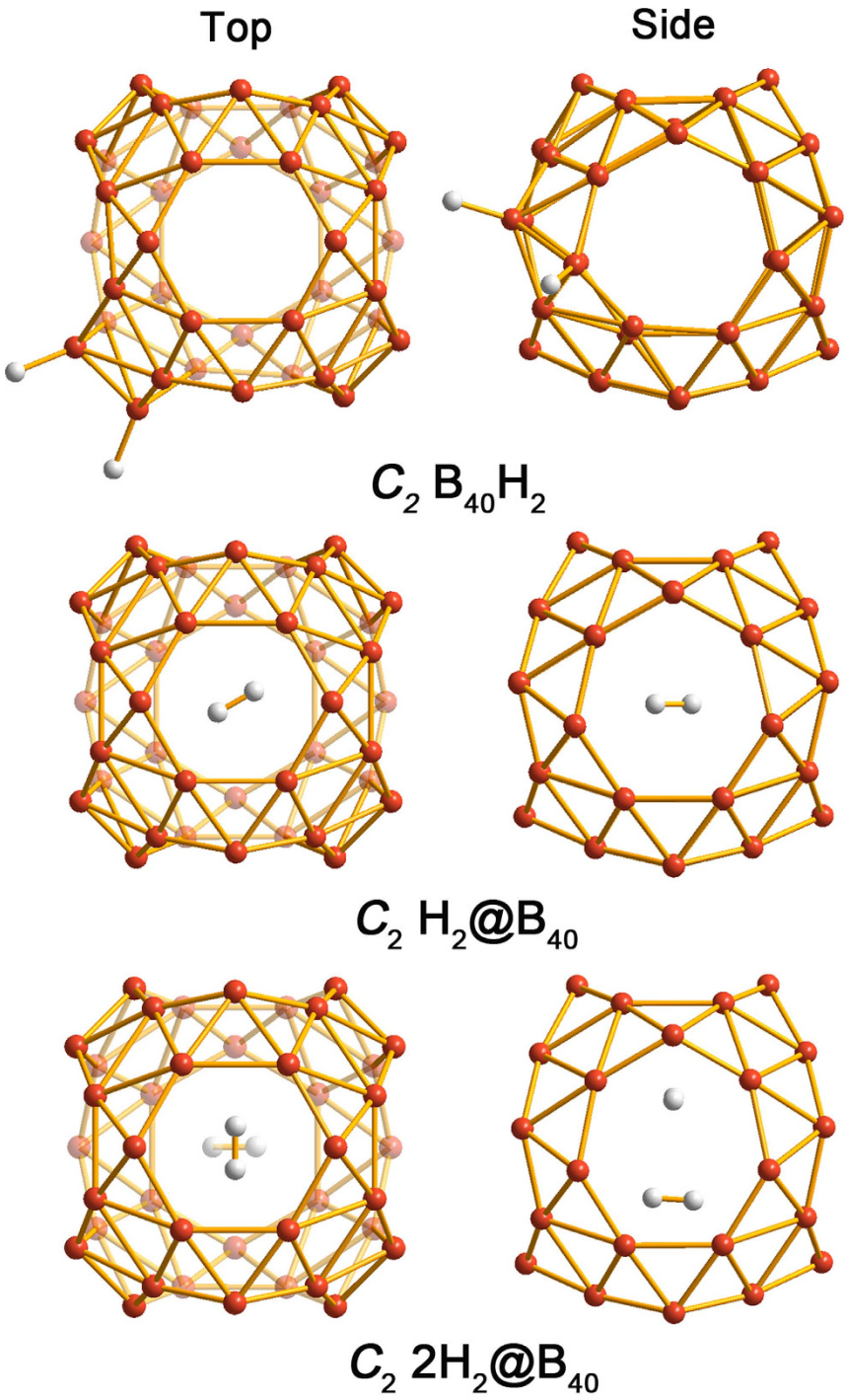

Figure 1. Top and side views of optimized configurations of $B_{40}H_2$, H_2@B_{40} and $2H_2$@B_{40}.

in Table 1, electron transfer occurs from Li to borospherene B_{40} cage in **1** and **2**, resulting in a positive charge of 0.87–0.88 |e| on Li as revealed in the Bader charge analysis. The ionized Li atom hints a possibility for H_2 adsorption via the polarization mechanism[18].

To increase the coverage of Li on B_{40}, we place one Li atom on top of every hexagon and heptagon hole and reach exohedral D_{2d} Li_6&B_{40}(**3**) (Fig. 2). In complex **3**, six Li atoms remain isolated on the surface holes, resulting in a highly symmetric D_{2d} geometry. The average BE of Li in **3** is 3.07 eV/Li, which is comparable to that in Li&B_{40}(**1**) (3.08 eV) and is slightly larger than that in Li&B_{40}(**2**) (2.88 eV). There appears to be a collective effect for Li adsorption because six Li atoms in **3** have a higher total BE (18.48 eV) than six individual Li atoms in **1** and **2** combined (18.08 eV). This fact suggests that Li_6&B_{40}(**3**) is a favorable configuration for Li-decoration. Remarkably but not surprisingly, our computational data indicate that **3** is at least 6.29 eV more stable than B_{40} attached by a compact Li_6 cluster (Fig. S1). Therefore, surface aggregation of Li for island clusters is unlikely in the

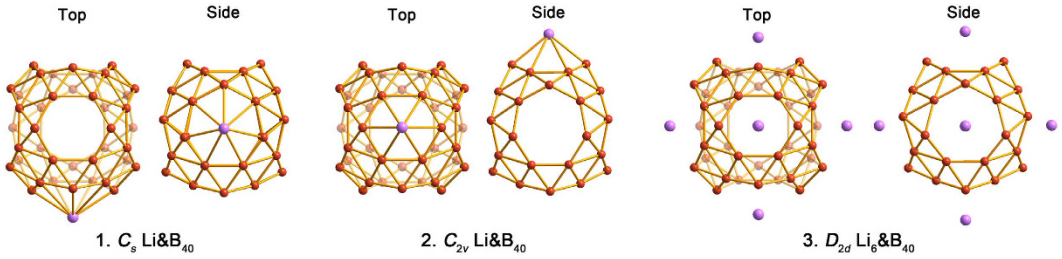

Figure 2. Top and side views of the optimized configurations of C_s Li&B$_{40}$(1), C_{2v} Li&B$_{40}$(2), and D_{2d} Li$_6$&B$_{40}$(3), in which one Li atom is coated on a heptagonal hole of B$_{40}$, one Li atom is on a hexagonal hole, and six Li atoms are on the heptagonal/hexagonal holes, respectively. The B atom is in orange and Li is in purple.

system	BE/Li (eV)	R_{Li-B} (Å)	charge on Li (|e|)
C_s Li&B$_{40}$(**1**)	3.08	2.34	0.88
C_{2v} Li&B$_{40}$(**2**)	2.88	2.33	0.87
D_{2d} Li$_6$&B$_{40}$(**3**)	3.07	2.33	0.87

Table 1. Calculated Binding Energy (BE) of Li to B$_{40}$, Li–B Bond Distance, and Atomic Charge on Li Atom for Li&B$_{40}$(1), Li&B$_{40}$(2), and Li$_6$&B$_{40}$(3).

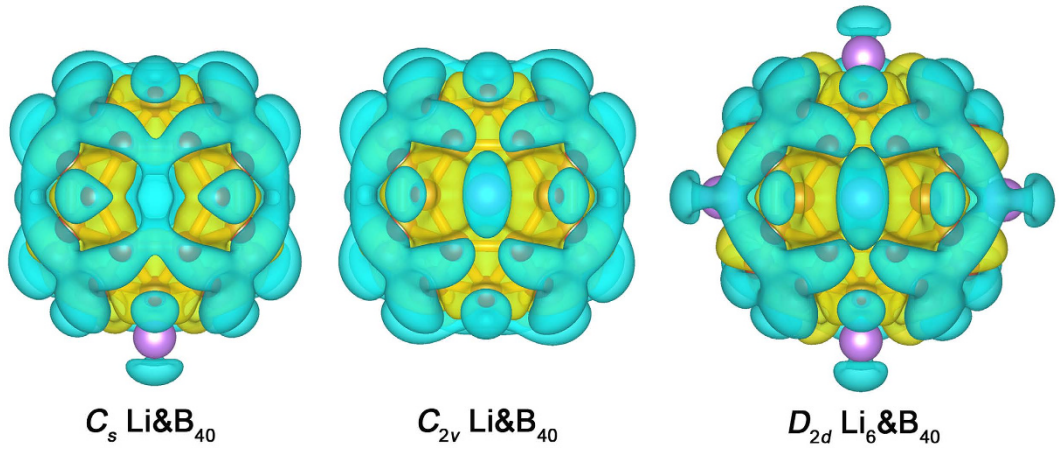

Figure 3. Top views of the isosurface of charge density differences of C_s Li&B$_{40}$(1), C_{2v} Li&B$_{40}$(2), and D_{2d} Li$_6$&B$_{40}$(3). Yellow color represents the electron accumulation region, and blue represents the electron depletion region.

Li$_6$&B$_{40}$ system. The Li–B distance in **3** is 2.33 Å, nearly identical to those in **1** and **2**. Bader charge analysis shows that the atomic charge on each Li atom in **3** is +0.87 |e|.

We further analyzed the isosurfaces of charge density differences in complexes C_s Li&B$_{40}$(**1**), C_{2v} Li&B$_{40}$(**2**), and D_{2d} Li$_6$&B$_{40}$(**3**), as depicted in Fig. 3. Here the yellow and blue colors represent electron accumulation and depletion regions, respectively. From the charge density variations of **1**–**3**, which are induced by the adsorption of Li atoms onto B$_{40}$, it is obvious that charge transfer from Li atom to B$_{40}$ indeed takes place upon Li decoration.

Figure 4 shows the frontier canonical molecular orbitals (CMOs) of **1**–**3**, which are compared with those of D_{2d} B$_{40}$. Upon attachment of the first Li atom on B$_{40}$, the lowest unoccupied molecular orbital (LUMO) of B$_{40}$ (Fig. 4d) becomes half-filled due to charge transfer, which are the singly occupied molecular orbitals (SOMOs) in **1** and **2** (Fig. 4a,b). Note these three CMOs are virtually identical. Likewise, in line with their lower symmetry, LUMO (a′) of **1** and LUMO (b_2) of **2** correspond to the degenerate LUMO + 1 of D_{2d} B$_{40}$. In D_{2d} Li$_6$&B$_{40}$(**3**) (Fig. 4c), six electrons are transferred from Li to the B$_{40}$ cage, which successively occupy the LUMO and degenerate LUMO + 1 of D_{2d} B$_{40}$. The latter LUMO + 1 become the highest occupied molecular orbital (HOMO) in **3**, which are also doubly degenerated due to the same high symmetry of D_{2d}. As a consequence, the LUMO + 2 (b_1) of D_{2d} B$_{40}$ becomes the LUMO in **3**. The spatial distributions of the frontier CMOs in these four species are remarkably similar, demonstrating the electronic robustness of the B$_{40}$ cage motif along this series. The calculated Wiberg bond indices associated with Li are all less than 0.30 in **1**–**3**, which further indicate that Li does not participate in the covalent bonding of B$_{40}$.

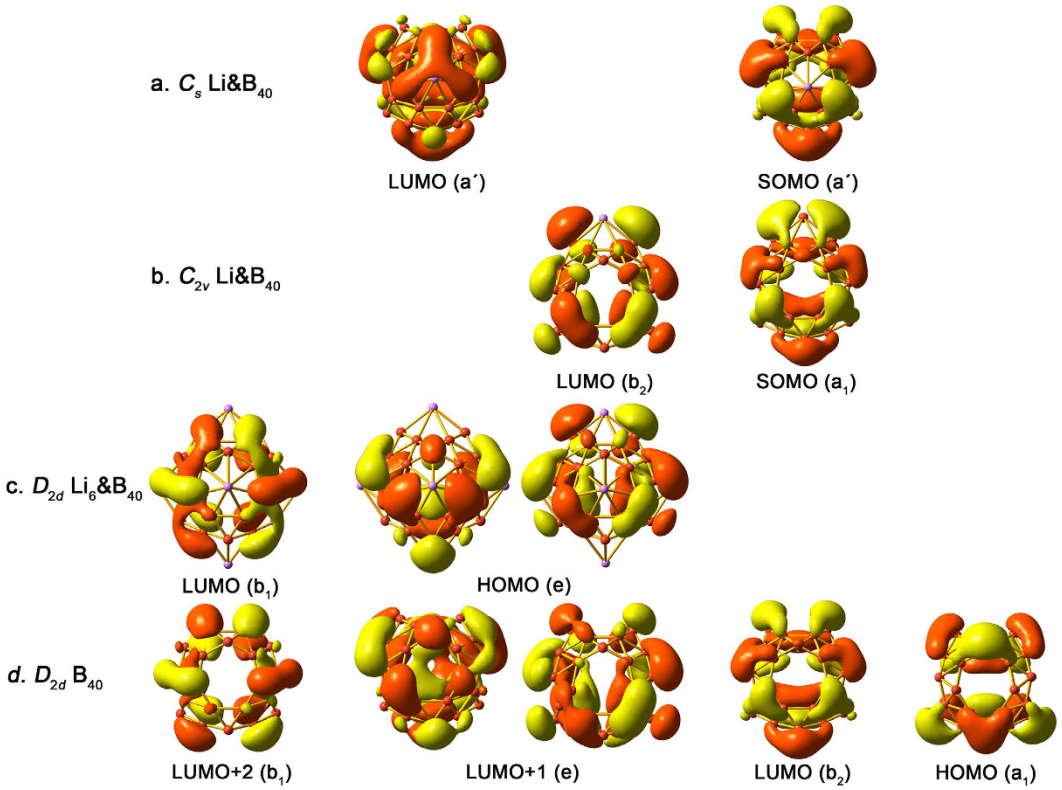

Figure 4. Molecular orbital pictures of the LUMOs and HOMOs (or SOMOs) of C_s Li&B$_{40}$(1), C_{2v} Li&B$_{40}$(2), and D_{2d} Li$_6$&B$_{40}$(3), as compared with those of borospherene D_{2d} B$_{40}$. The orbitals are aligned according to their shapes.

The calculated HOMO-LUMO energy gaps of **1**, **2**, and **3** are 1.39, 1.41, and 1.42 eV, respectively, which differ from that of D_{2d} B$_{40}$ (3.13 eV at the same level), suggesting the possibility to tune the electronic properties of borospherenes via metal-decoration, similar to the case of C_{60} buckyball.

H_2 Adsorption on Li-Decorated B_{40}. The C_s Li&B$_{40}$(**1**), C_{2v} Li&B$_{40}$(**2**), and D_{2d} Li$_6$&B$_{40}$(**3**) clusters are well-defined molecular systems for the adsorption of H_2 molecules. H_2 can be added successively to the systems, from one H_2 molecule up to six per Li site. The largest complex corresponds to the adsorption of 34 H_2 molecules to **3**, that is, Li$_6$&B$_{40}$(**3**)-34 H_2. Tables S1 and 2 summarize the AEs and the equilibrium Li–B, Li–H, and H–H distances for the Li$_m$-B$_{40}$-nH$_2$ ($m = 1, 6$; $n = 1$–34) complexes.

When one H_2 molecule is introduced to **1**, due to the polarization interaction between the charged Li atom and the H_2 molecule, the Li–B bond distance is slightly enlarged (by 0.01 Å) to 2.35 Å. The H–H distance is found to be 0.76 Å. The equilibrium Li–H distance is 1.97 Å, which is comparable to the value of 2.04 Å in the case of a free Li^+ ion interacting with H_2[46]. The AE of the first H_2 to **1** is 0.25 eV, which is in quantitative agreement with that in Li^+H_2 (0.25 eV)[46].

With more H_2 molecules being attached to **1**, the average AE of H_2, consecutive AE of H_2, the Li–B distance, and the distances between H_2 and Li change accordingly. As shown in Table S1 and Fig. 5a, a single Li atom in **1**, coated on a heptagonal hole, can adsorb up to six H_2 molecules with an average AE of 0.11 eV/H_2. From one to six H_2, the average AE decreases from 0.25 to 0.11 eV/H_2, whereas the consecutive AE decrease from 0.25 to 0.05 eV/H_2. This effect may be partially due to the steric repulsion[47] when the number of H_2 molecules increases. In line with this trend, the Li–B distances are elongated gradually from 2.35 to 2.43 Å. However, the H–H bond distance is nearly constant in the range of 0.75–0.76 Å, which is the value of free H_2 molecule, consistent with the nature of molecular adsorption. The Li–H distances span a rather wide range from 1.97 to 2.91 Å. Notably, there is an abrupt increase in the Li–H distances from **1**–3 H_2 to **1**–4 H_2, so that the first three H_2 are closer to the Li site than the next three. In other words, the adsorption of the first three H_2 molecules forms an inner core with Li, upon which the additional H_2 molecules adsorb loosely. The data of consecutive AE confirm this to be indeed the case: The first three H_2 possess an AE of 0.25–0.11 eV, in contrast to 0.04–0.05 eV for the next three (Table S1). In fact, the structure of **1**–4 H_2 can be constructed on the basis of **1**–3 H_2 by adding one H_2 on the top of Li. However, when the fifth and sixth H_2 are put on successively in **1**–5 H_2 and **1**–6 H_2, they flee away after structural optimization as shown in Fig. 5a. Therefore, the Li site in **1** may adsorb three H_2 molecules comfortably, whereas additional H_2 are only physisorbed.

Basically, the adsorption of H_2 on **2** is rather similar to that on **1**. Up to five H_2 molecules may be adsorbed on the Li site in **2** (Fig. 5b). Again, the first three H_2 are located closely to Li, with the fourth H_2 being situated symmetrically on top of Li at a substantially larger distance. For the **2**–5 H_2 case, there is a structural rearrangement

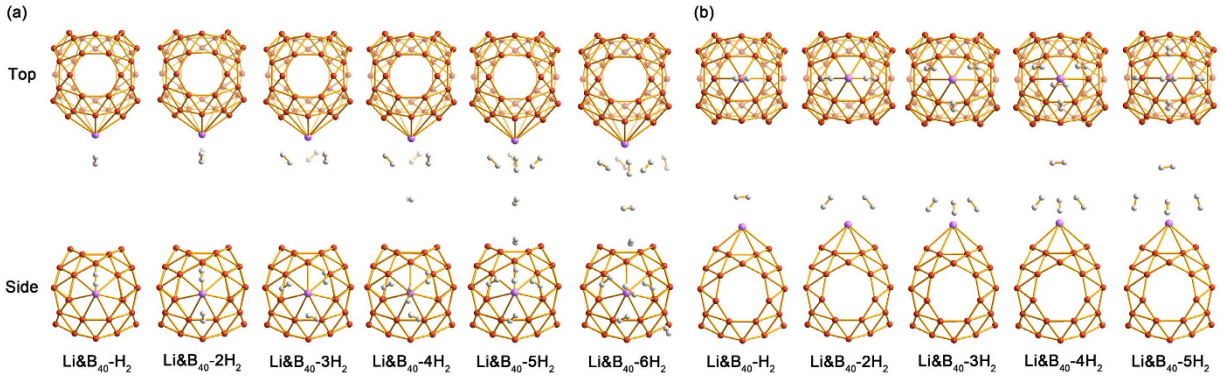

Figure 5. Top and side views of the optimized configurations for successive addition of H_2 molecules on (**a**) Li&B_{40}(**1**) with a Li-coated heptagonal hole and (**b**) Li&B_{40}(**2**) with a Li-coated hexagonal hole.

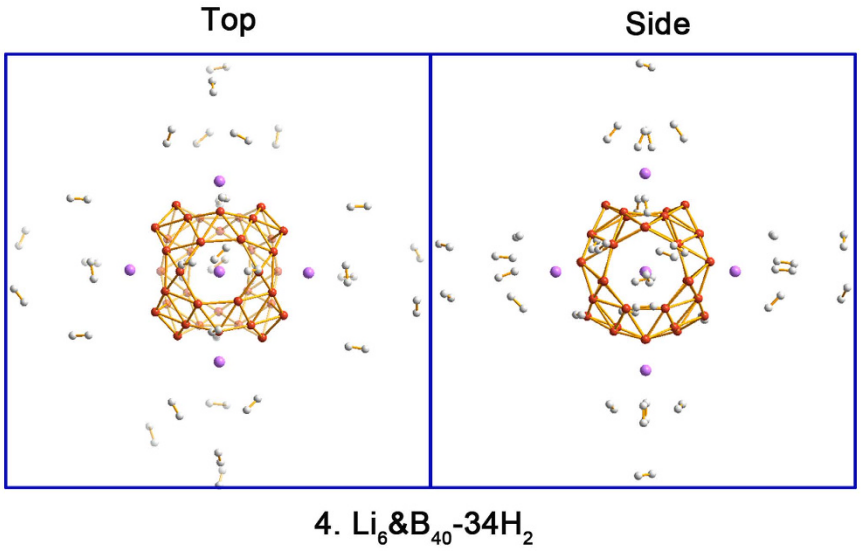

Figure 6. Top and side views of the optimized configuration of Li_6&B_{40}-34 H_2(4). The B atom is in orange, Li in purple, and H in white.

for the H_2 molecules, suggesting that this Li site can potentially adsorb up to four H_2 molecules at a reasonable strength. Nonetheless, the fifth H_2 only interact with Li loosely. On the basis of the consecutive AEs (0.22–0.17 eV for the first three H_2; Table S1), we conclude that the Li site in **2** is capable of adsorbing at least three H_2 molecules with further possibility for a fourth, whereas additional H_2 molecules should be considered physisorbed.

Based on the above results of H_2 adsorption on single Li-decorated B_{40}, we constructed and optimized the H_2 adsorption configurations on the Li_6&B_{40}(**3**) complex, which aims at exploring the hydrogen storage capacity. The starting configurations were constructed by attaching the corresponding H_2 molecules around Li atoms above the 4 heptagonal and 2 hexagonal holes on the B_{40} cage. Successively, 6 H_2, 12 H_2, 18 H_2, 24 H_2, and up to 34 H_2 are adsorbed on Li_6&B_{40}(**3**), whose optimized structures are shown in Fig. S2 and 6. The former four cases correspond to the adsorption of one to four H_2 on each Li site. For the 34 H_2 case, that is, Li_6&B_{40}-34 H_2(**4**), 6 H_2 are adsorbed on each heptagonal Li site and 5 H_2 are on each hexagonal Li site, as depicted in Fig. 6. The total interaction energy of 34 H_2 in **4** is 3.43 eV, yielding an average AE of 0.10 eV/H_2. The calculated consecutive AEs are collected in Table 2, which reflects the adsorption nature more faithfully. Similar to **1** and **2**, the first three H_2 for each Li in **4** are located close to the adsorption site, resulting in the **3**–6 H_2, **3**–12 H_2, and **3**–18 H_2 complexes with reasonable AEs of 0.18–0.11 eV/H_2. Additional H_2 molecules in **3**–24 H_2 and **4** complexes are farther away for the Li sites with relatively weak AEs of 0.03–0.05 eV/H_2, hinting physisorption in nature. In summary, up to 34 H_2 molecules may be adsorbed in **4**, among which the first 18 interact in moderate strength with the Li site, corresponding to a gravimetric density of 7.1 wt%.

H_2 Adsorption on Li-Decorated $B_{40}H_{16}$. Borospherene B_{40} as an electron-deficient system[36] is generally considered to be more reactive than C_{60}, we can thus engineer and passivate B_{40} at least partially with B–H bonds, which may benefit the adsorption and release of H_2 molecules. B_{40} has 16 tetracoordinate and 24 pentacoordinate sites, where the former are anticipated to be more reactive. A model $B_{40}H_{16}$ cage cluster is readily constructed via

system	AE/H_2(eV) (average)	AE/H_2 (eV) (consecutive)	R_{Li-B} (Å)	R_{Li-H} (Å)	R_{H-H} (Å)
Li_6&B_{40}-6 H_2	0.18	0.18	2.34	1.99	0.75
Li_6&B_{40}-12 H_2	0.17	0.17	2.37	2.00	0.76
Li_6&B_{40}-18 H_2	0.15	0.11	2.41	2.08	0.76
Li_6&B_{40}-24 H_2	0.12	0.03	2.41	2.54	0.76
Li_6&B_{40}-34 H_2	0.10	0.05	2.42	2.94	0.76

Table 2. Calculated Average and Consecutive Adsorption Energy (AE) of H_2, Bond Distances of Li–B, Li–H, and H–H in the Li_6&B_{40}-nH_2 ($n = 6, 12, 18, 24, 34$) Complexes.

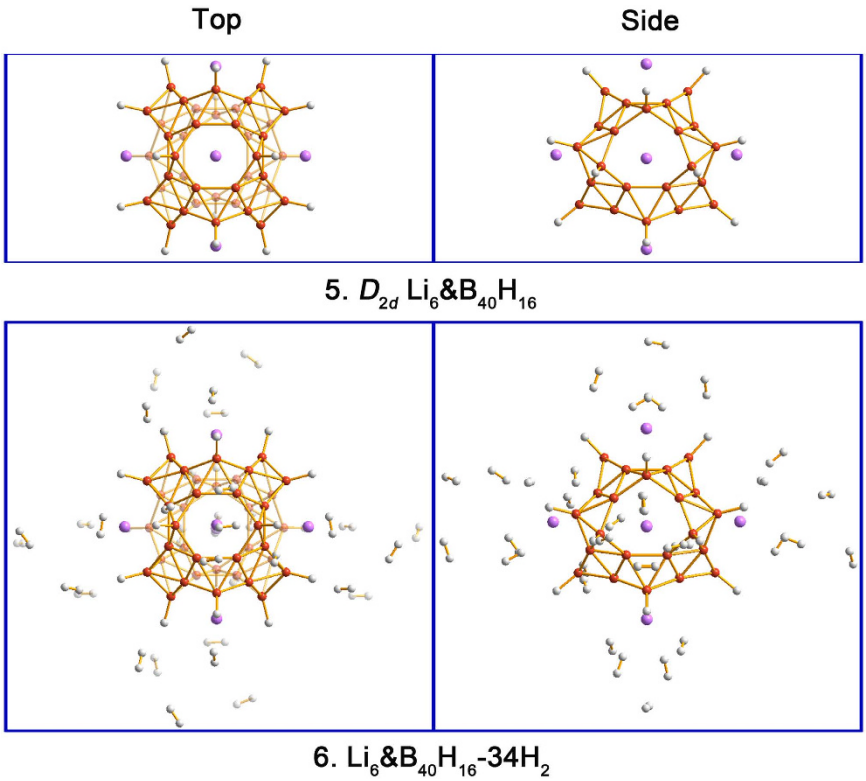

Figure 7. Top and side views of the optimized configurations of Li_6&$B_{40}H_{16}$(5) and Li_6&$B_{40}H_{16}$-34 H_2(6). The B atom is in orange, Li in purple, and H in white.

16 B–H bonds for the tetracoordinate B sites, which can also be decorated with six Li atoms, resulting in a D_{2d} Li_6&$B_{40}H_{16}$(**5**) complex as depicted in Fig. 7. The Li–B distance in **5** remains to be 2.33 Å, which is very close to that in **3**. In complex **5**, each Li atom carries a charge of 0.88 |e|. Interestingly, the B–H bonds markedly alter the Li-decoration properties in **5** and the average BE of Li atom now increases to 4.17 eV per Li, compared to 3.07 eV in Li_6&B_{40}(**3**).

Li_6&$B_{40}H_{16}$(**5**) can also adsorb from 6 H_2, 12 H_2, 18 H_2, 24 H_2, and up to 34 H_2 molecules, resulting in a series of **5**-nH_2 complexes (Fig. S3). The optimized structure for Li_6&$B_{40}H_{16}$-34 H_2(**6**) is shown in Fig. 7. Note that hydrogen remains in the molecular state with a uniform H–H distance of 0.75 Å in all **5**-nH_2 species. For the first 6 H_2 molecules in **5**–6 H_2, the average AE amounts to 0.22 eV/H_2. The average Li–B and Li–H distances, 2.33 and 1.97 Å, respectively, are almost the same as those in Li_6&B_{40}-6 H_2 (that is, **3**–6 H_2). With further H_2 adsorption, the average AEs for the first 18 H_2 in **5**-nH_2 decrease slightly down to 0.17 eV/H_2, which are in the ideal thermodynamic range for reversible hydrogen storage[10,11]. The Li_6&$B_{40}H_{16}$(**5**) complex thus behaves rather similar to Li_6&B_{40}(**3**) in terms of hydrogen storage properties, except for the B–H passivation in **5**. The 18 "core" H_2 in Li_6&$B_{40}H_{16}$-34 H_2(**6**) represents a gravimetric density of 6.5 wt%, where an additional 8.6 wt% of dissociated H atoms and loosely physisorbed 16 H_2 are not counted.

On the Possibility of Doubling the H_2 Adsorption Sites: Li-Decorated Triangular B_6 Corners. To further improve the hydrogen storage capacity of Li-decorated B_{40}, we also attempted to place Li atoms on top of the close-packing, triangular B_6 corner sites of the cube-like B_{40} cage. As a test case, adsorption of a single H_2 molecule on a corner Li site is optimized (Fig. S4). The BE of Li is 1.87 eV, which is lower than those in Li&B_{40}(**1**) and Li&B_{40}(**2**), but the value still represents a reasonable strength. In fact, it is comparable to the corresponding value for C_{60} (1.80 eV)[13]. Moreover, the AE for the first H_2 amounts to 0.28 eV, which is comparable to and even slightly

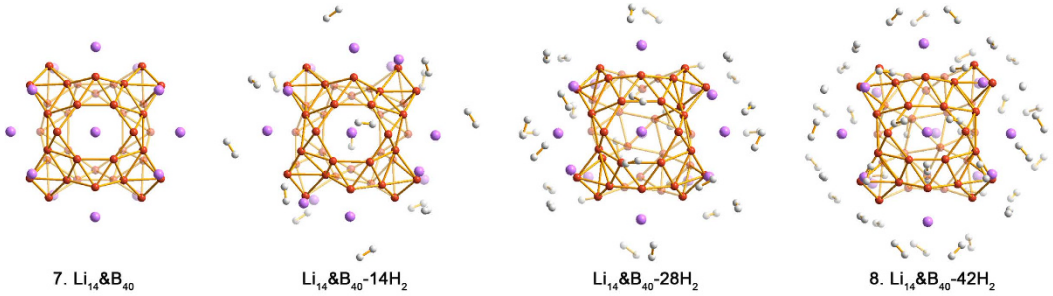

Figure 8. Optimized configurations of $Li_{14}\&B_{40}$(7) and its H_2 adsorption complexes: $Li_{14}\&B_{40}$-14 H_2, $Li_{14}\&B_{40}$-28 H_2, and $Li_{14}\&B_{40}$-42 H_2(8). The B atom is in orange, Li in purple, and H in white.

greater than that in Li&B_{40}(**1**)-H_2 (0.25 eV) or Li&B_{40}(**2**)-H_2 (0.22 eV; Table S1). The above data hint that a triangular B_6 corner site on B_{40} is as promising as, if not better than, a hexagonal/heptagonal site for hydrogen storage. The calculated consecutive AEs of Li&B_{40}-nH_2 (n = 1–3) with H_2 molecules adsorbed on a corner Li site are at the range of 0.22–0.28 eV/H_2. For $Li_8\&B_{40}$-nH_2 (n = 8, 16, 24) with H_2 molecules adsorbed on eight corner Li site, the consecutive AEs change from 0.17 to 0.36 eV/H_2, which are ideal for reversible hydrogen storage and release

In this way, one can more than double the number of sites for Li-decoration from six in $Li_6\&B_{40}$(**3**) and $Li_6\&B_{40}H_{16}$(**5**) to fourteen in $Li_{14}\&B_{40}$(**7**), owing to the eight triangular B_6 corners (versus six hexagonal/heptagonal holes). The optimized structure of $Li_{14}\&B_{40}$(**7**) is shown in Fig. 8. Here, upon Li decoration, the boron structure distorts considerably from the free-standing B_{40} borospherene, but the cage motif maintains. The average BE is 2.57 eV/Li. Following the strategy for $Li_6\&B_{40}$(**3**) and $Li_6\&B_{40}H_{16}$(**5**), we build a series of model complexes: **7**–14 H_2, **7**–28 H_2, and $Li_{14}\&B_{40}$-42 H_2(**8**), whose optimized structures are depicted in Fig. 8. The calculated average AE for the first 14 H_2 in **7**–14 H_2 is 0.32 eV/H_2, for the second 14 H_2 in **7**–28 H_2 is 0.22 eV/H_2, and for the third 14 H_2 in $Li_{14}\&B_{40}$-42 H_2(**8**) is 0.12 eV/H_2, suggesting that all these H_2 molecules are thermodynamically favorable for a hydrogen storage material[10,11]. For the extreme case of **8**, a maximum gravimetric density of 13.8 wt% is obtained. We do not exclude the possibility of further H_2 adsorption onto the **8** complex, albeit those additional H_2 are anticipated to interact rather loosely with the Li sites.

Concluding Remarks

In conclusion, we have carried out a comprehensive density-functional study on the lithium-decoration of B_{40} borospherene and the potential utilization of Li-B_{40} complexes as a novel nanomaterial for hydrogen storage. We showed that all six heptagonal and hexagonal holes on B_{40} surface can be decorated with Li atoms and each Li site is capable of adsorbing up to six or five H_2 molecules. This results in an ultimate $Li_6\&B_{40}$-34 H_2 complex, in which 18 H_2 are bound to Li sites with ideal adsorption energies of 0.11–0.18 eV per H_2, corresponding to a gravimetric density of 7.1 wt%. The additional 16 H_2 are physisorbed in nature. We further showed that the eight close-packing, triangular B_6 corner sites on the B_{40} cage are also readily decorated with Li, which more than double the number of sites for hydrogen storage. The corresponding $Li_{14}\&B_{40}$-42 H_2 complex can store all 42 H_2 molecules at adsorption energies of 0.12–0.32 eV per H_2, suggesting a maximum gravimetric density of 13.8 wt%. The Li-B_{40}-H_2 complexes as a hydrogen storage material differ markedly from the prior Li-C_{60}-H_2 and Ti-B_{40}-H_2 systems. The Li-C_{60}-H_2 complex[13] adsorbs H_2 rather loosely and is thus not efficient for hydrogen storage, whereas the Ti-B_{40}-H_2 complex[40] bounds H_2 too strongly, for which a substantial portion of H_2 stored are not reversible for release. In fact, preliminary attempts also suggest that the structural integrity of B_{40} unit is maintained when they are allowed to interact with each other. Considering the presence of chemical bondings between them, we forecast it is possible to construct boron-based nanomaterials for hydrogen storage using lithium-decorated B_{40} unit as a building block or connecting the exohedral metalloborospherene with organic linkers. And the hydrogen storage capacity of the boron-based nanomaterials could be better than previously reported carbon-based counterparts.

Methods

All calculations were based on DFT, using a plane-wave basis set with the Projector Augmented Wave (PAW)[48,49] pseudopotential method as implemented in the Vienna *ab initio* Simulation Package (VASP)[50,51]. Generalized gradient approximation (GGA) with the Perdew-Burke-Ernzerhof (PBE)[52] functional was adopted to treat the electron exchange correlation. The GGA-PBE method has been previously utilized to treat Li-decorated fullerenes and heterofullerenes for hydrogen storage[19,53] which is thus a suitable choice for our current system. The dispersion corrected DFT (DFT-D) scheme[54–56] was used to describe the van der Waals (vdW) interaction. The supercell approach was used, where the B_{40}-based systems were placed at the center of a $25 \times 25 \times 25$ Å^3 vacuum space. And only the Γ point was used to sample the Brillouin zone. The energy cutoff for the plane-wave basis set was set to 500 eV. All structures were fully relaxed until the force acting on each atom was less than 10^{-2} eV/Å and a tolerance in total energy was at least 10^{-4} eV.

The binding energies (BEs) for the Li-decorated B_{40} are defined as $E_b = -(E_{Li\text{-}B40} - E_{B40} - mE_{Li})/m$, where $E_{Li\text{-}B40}$ is the total energy of Li-decorated B_{40}, E_{B40} and E_{Li} are the total energies of an isolated B_{40} and a Li atom, respectively, and m is the number of Li atoms. Similarly, the average AE for H_2 is defined as $E_a = -(E_{Li\text{-}B40\text{-}nH2} - E_{Li\text{-}B40} - nE_{H2})/n$ and the consecutive AE is defined as $\Delta E = -(E_{Li\text{-}B40\text{-}nH2} - E_{Li\text{-}B40\text{-}(n\text{-}1)H2} - E_{H2})$, where $E_{Li\text{-}B40\text{-}nH2}$ and $E_{Li\text{-}B40\text{-}(n\text{-}1)H2}$ are the total energies of n and (n–1) H_2 adsorbed on the Li-decorated B_{40}, respectively. $E_{Li\text{-}B40}$ also represents the total energy

of Li-decorated B_{40}, E_{H2} is the total energy of isolated H_2 molecule, and *n* stands for the number of adsorbed H_2 molecules.

We note that for comparison with D_{2d} B_{40} in our previous work (ref. 36), the HOMO-LUMO energy gaps of **1**, **2**, and **3** were calculated using the Gaussian 09 package[57], which is usually used for calculations on the isolated molecules. And the corresponding structures were optimized at the PBE0 levels with the 6–311 + G* basis set[58,59], which has been benchmarked in prior works as a reliable method for boron clusters.

References

1. Schlapbach, L.& Züttel, A. Hydrogen-storage materials for mobile applications. *Nature* **414,** 353–358 (2001).
2. Cortright, R. D., Davada, R. R. & Dumesic, J. A. Hydrogen from catalytic reforming of biomass- derived hydrocarbons in liquid water. *Nature* **418,** 964–967 (2002).
3. Coontz, R. & Hanson, B. Not So Simple. *Science* **305,** 957 (2004).
4. Lubitz, W. & Tumas, W. Hydrogen: an overview. *Chem. Rev.* **107,** 3900–3903 (2007).
5. Dresselhaus, M. S. & Thomas, I. L. Alternative energy technologies. *Nature* **414,** 332–337 (2001).
6. Crabtree, G. W., Dresselhaus, M. S. & Buchanan, V. The hydrogen economy. *Phys. Today* **57,** 39–44 (2004).
7. Eberle, U., Felderhoff, M. & Schüth, F. Chemical and physical solutions for hydrogen storage. *Angew. Chem., Int. Ed*. **48,** 6608–6630 (2009).
8. Cohen, R. L. & Wernick, J. H. Hydrogen storage materials: properties and possibilities. *Science* **214,** 1081–1087 (1981).
9. Graetz, J. New approaches to hydrogen storage. *Chem. Soc. Rev.* **38,** 73–82 (2009).
10. Meng, S., Kaxiras, E. & Zhang, Z. Metal-diboride nanotubes as high-capacity hydrogen storage media. *Nano Lett*. **7,** 663–667 (2007).
11. Murray, L. J., Dincă, M. & Long, J. R. Hydrogen storage in metal–organic frameworks. *Chem. Soc. Rev.* **38,** 1294–1314 (2009).
12. Chandrakumar, K. R. S. & Ghosh, S. K. Alkali-metal-induced enhancement of hydrogen adsorption in C_{60} fullerene: an *ab Initio* study. *Nano Lett*. **8,** 13–19 (2008).
13. Sun, Q., Jena, P., Wang, Q. & Marquez, M. First-principles study of hydrogen storage on $Li_{12}C_{60}$. *J. Am. Chem. Soc.* **128,** 9741–9745 (2006).
14. Wang, Q., Sun, Q., Jena, P. & Kawazoe, Y. Theoretical study of hydrogen storage in Ca-coated fullerenes. *J. Chem. Theory Comput.* **5,** 374–379 (2009).
15. Teprovich, Jr. J. A. *et al.* Synthesis and characterization of a lithium-doped fullerane (Li_x-C_{60}-H_y) for reversible hydrogen storage. *Nano Lett*. **12,** 582–589 (2012).
16. Mauron, P. *et al.* Hydrogen sorption in $Li_{12}C_{60}$, *J. Phys. Chem. C* **117,** 22598−22602 (2013).
17. Yoshida, A. *et al.* Reversible hydrogen storage/release phenomena on lithium fulleride (Li_nC_{60}) and their mechanistic investigation by solid-state NMR spectroscopy. *J. Mater. Chem.* **21,** 9480−9482 (2011).
18. Yoon, M. *et al.* Calcium as the superior coating metal in functionalization of carbon fullerenes for high-capacity hydrogen storage. *Phys. Rev. Lett.* **100,** 206806 (2008).
19. Wang, Q. & Jena, P. J. Density functional theory study of the interaction of hydrogen with Li_6C_{60}. *Phys. Chem. Lett.* **3,** 1084–1088 (2012).
20. Sun, Q., Wang, Q. & Jena, P. Storage of molecular hydrogen in BN cage: energetics and thermal stability. *Nano Lett*. **5,** 1273–1277 (2005).
21. Kim, Y. H. *et al.* Nondissociative adsorption of H_2 molecules in light-element-doped fullerenes. *Phys. Rev. Lett.* **96,** 016102 (2006).
22. Zhao, Y. F. *et al.* Boron-based organometallic nanostructures: hydrogen storage properties and structure stability. *Nano Lett*. **8,** 157–161 (2008).
23. Yildirim, T. & Ciraci, S. Titanium-decorated carbon nanotubes as a potential high-capacity hydrogen storage medium. *Phys. Rev. Lett.* **94,** 175501 (2005).
24. Fakioğlu, E., Yürüm, Y. & Veziroğlu, T. N. A review of hydrogen storage systems based on boron and its compounds. *Int. J. Hydrogen Energ.* **29,** 1371–1376 (2004).
25. Orimo, S. I. *et al.* Complex hydrides for hydrogen storage. *Chem. Rev.* **107,** 4111–4132 (2007).
26. Hazrati, E., Brocks, G. & de Wijs, G. A. First-principles study of $LiBH_4$ nanoclusters and their hydrogen storage properties. *J. Phys. Chem. C* **116,** 18038–18047 (2012).
27. Li, M. *et al.* Ca-coated boron fullerenes and nanotubes as superior hydrogen storage materials. *Nano Lett*. **9,** 1944–1948 (2009).
28. Er, S., de Wijs, G. A. & Brocks, G. DFT study of planar boron sheets: a new template for hydrogen storage. *J. Phys. Chem. C* **113,** 18962–18967 (2009).
29. Wang, J., Zhao, H. Y. & Liu, Y. Boron-double-ring sheet, fullerene, and nanotubes: potential hydrogen storage materials. *ChemPhysChem* **15,** 3453–3459 (2014).
30. Szwacki, N. G., Sadrzadeh, A. & Yakobson, B. I. B_{80} fullerene: an *ab initio* prediction of geometry, stability, and electronic structure. *Phys. Rev. Lett.* **98,** 166804 (2007).
31. Li, Y. C. *et al.* Alkali-metal-doped B_{80} as high-capacity hydrogen storage media. *J. Phys. Chem. C* **112,** 19268–19271 (2008).
32. Wu, G. F., Wang, J. L., Zhang, X. Y. & Zhu, L. Y. Hydrogen storage on metal-coated B_{80} buckyballs with density functional theory. *J. Phys. Chem. C* **113,** 7052–7057 (2009).
33. Li, J. L., Hu, Z. S. & Yang, G. W. High-capacity hydrogen storage of magnesium-decorated boron fullerene. *Chem. Phys.* **392,** 16–20 (2012).
34. Li, F. Y. *et al.* B_{80} and $B_{101-103}$ clusters: remarkable stability of the core-shell structures established by validated density functionals. *J. Chem. Phys.* **136,** 074302 (2012).
35. Goedecker, S., Hellmann, W. & Lenosky, T. Global minimum determination of the born- oppenheimer surface within density functional theory. *Phys. Rev. Lett.* **95,** 055501 (2005).
36. Zhai, H. J. *et al.* Observation of an all-boron fullerene. *Nature Chem*. **6,** 727–731 (2014).
37. Bai, H., Chen, Q., Zhai, H. J. & Li, S. D. Endohedral and exohedral metalloborospherenes: M@B_{40} (M = Ca, Sr) and M&B_{40} (M = Be, Mg). *Angew. Chem., Int. Ed.* **54,** 941–945 (2015).
38. Chen, Q. *et al.* Experimental and theoretical evidence of an axially chiral borospherene. *ACS Nano* **9,** 754–760 (2015).
39. Chen, Q. *et al.* Cage-like B_{41}^+ and B_{42}^{2+}: new chiral members of the borospherene family. *Angew. Chem., Int. Ed*. **54,** 8160–8164 (2015).
40. Dong, H. L., Hou, T. J., Lee, S. T. & Li, Y. Y. New Ti-decorated B_{40} fullerene as a promising hydrogen storage material. *Sci. Rep*. **5,** 09952 (2015).
41. Targets for onboard hydrogen storage systems for light-duty vehicles, US Department of Energy Office of Energy Efficiency and Renewable Energy and The FreedomCAR and Fuel Partnership, (2009).
42. Churchard, A. J. *et al.* A multifaceted approach to hydrogen storage. *Phys. Chem. Chem. Phys.* **13,** 16955–16972 (2011).
43. Srinivasu, K. & Ghosh, S. K. An *ab Initio* investigation of hydrogen adsorption in li-doped *closo*-boranes. *J. Phys. Chem. C* **115,** 1450–1456 (2011).
44. Tai, T. B. & Nguyen, M. N. A three-dimensional aromatic B_6Li_8 complex as a high capacity hydrogen storage material. *Chem. Commun.* **49,** 913–915 (2013).

45. Pupysheva, O. V., Garajian, A. A. & Yakobson, B. I. Fullerene nanocage capacity for hydrogen storage. *Nano Lett*. **8,** 767–774 (2008).
46. Rao, B. K. & Jena, P. Hydrogen uptake by an alkali metal ion. *Europhys. Lett.* **20,** 307–312 (1992).
47. Pophristic, V. & Goodman, L. Hyperconjugation not steric repulsion leads to the staggered structure of ethane. *Nature* **411,** 565–568 (2001).
48. Blochl, P. E. Projector augmented-wave method. *Phys. Rev. B* **50,** 17953–17979 (1994).
49. Kresse, G. & Joubert, D. From ultrasoft pseudopotentials to the projector augmented-wave method. *Phys. Rev. B* **59,** 1758–1775 (1999).
50. Kresse, G. & Hafner, J. Norm-conserving and ultrasoft pseudopotentials for first-row and transition elements. *J. Phys.: Condens. Matter* **6,** 8245–8257 (1994).
51. Kresse, G. & Furthmuller, J. Efficient iterative schemes for *ab initio* total-energy calculations using a plane-wave basis set. *Phys. Rev. B* **54,** 11169–11186 (1996).
52. Perdew, J. P., Burke, K. & Ernzerhof, M. Generalized gradient approximation made simple. *Phys. Rev. Lett.* **77,** 3865–3868 (1996).
53. Gao, Y., Wu, X. J. & Zeng, X. C. Designs of fullerene-based frameworks for hydrogen storage. *J. Mater. Chem. A* **2,** 5910–5914 (2014).
54. Wu, Q. & Yang, W. Empirical correction to density functional theory for van der waals interactions. *J. Chem. Phys.* **116,** 515–524 (2002).
55. Ortmann, F., Bechstedt, F. & Schmidt, W. G. Semiempirical van der waals correction to the density functional description of solids and molecular structures. *Phys. Rev. B*. **73,** 205101 (2006).
56. Johnson, E. R., Mackie, I. D. & DiLabio, G. A. Dispersion interactions in density-functional theory. *J. Phys. Org. Chem.* **22,** 1127–1135 (2009).
57. Frisch, M. J. *et al. Gaussian 09, Revision B.01* Gaussian, Inc., Wallingford, CT (2010).
58. Adamo, C. & Barone, V. Toward reliable density functional methods without adjustable parameters: the PBE0 model. *J. Chem. Phys.* **110,** 6158–6170 (1999).
59. Krishnan, R., Binkley, J. S., Seeger, R. & Pople, J. A. Self-consistent molecular orbital methods. XX. A basis set for correlated wave functions. *J. Chem. Phys.* **72,** 650–654 (1980).

Acknowledgements

This work was supported by the Key Projects of the National Natural Science Foundation of China (No. 21336006), the National Key Technology R&D Program (No. 2013BAC14B04), the National Natural Science Foundation of China (No. 21573138 and 21243004), the Shanxi Province Science Foundation for Youths (No. 201601D202017), the Youth Foundation of Taiyuan University of Technology (No. 1205-04020202), the Scientific Research Fund for the Introduction of Talents from Taiyuan University of Technology (No. tyut-rc201519a), and the State Key Laboratory of Quantum Optics and Quantum Optics Devices (No. KF201402).

Author Contributions

H.B., W.H., H.-J.Z. and S.-D.L. designed the project. H.B., B.B., L.Z. and Y.-W.M. constructed the structures and performed the electronic structure calculations. B.B. and L.Z. prepared all the figures and tables. H.B., W.H., H.-J.Z. and S.-D.L. analysed the data and wrote the paper. All authors discussed the results and made comments and edits to the manuscript.

Additional Information

Supplementary information accompanies this paper at http://www.nature.com/srep

Competing financial interests: The authors declare no competing financial interests.

How to cite this article: Bai, H. *et al.* Lithium-Decorated Borospherene B_{40}: A Promising Hydrogen Storage Medium. *Sci. Rep.* **6**, 35518; doi: 10.1038/srep35518 (2016).